

Diffusion of Cs, Np, Am and Co in compacted sand-bentonite mixtures: evidence for surface diffusion of Cs cations[†]

T. SAWAGUCHI^{1,*}, T. YAMAGUCHI¹, Y. IIDA¹, T. TANAKA¹
AND I. KITAGAWA²

¹ Waste Safety Research Group, Nuclear Safety Research Center, Japan Atomic Energy Agency, Tokai, Ibaraki 319-1195, Japan, and ² Hot Material Examination Section, Department of Fukushima Technology Development, Japan Atomic Energy Agency, Tokai, Ibaraki 319-1195, Japan

(Received 4 December 2012; revised 29 March 2013; Editor: John Adams)

ABSTRACT: We studied the diffusive transport of Cs, Np, Am and Co in compacted sand-bentonite mixtures by using the through-diffusion method. The experiments for Cs were performed under various aqueous compositions. Effective diffusivity (D_e) values of 4.7×10^{-10} to $5.9 \times 10^{-9} \text{ m}^2 \text{ s}^{-1}$ were obtained with a somewhat large variation. Apparent diffusivity (D_a) values, on the other hand, showed less variation, ranging from 2.0×10^{-12} to $6.2 \times 10^{-12} \text{ m}^2 \text{ s}^{-1}$. The results indicated that diffusive flux was proportional to the concentration gradient on the basis of the amount of Cs in the unit volume of the compacted sand-bentonite mixtures rather than the Cs concentration gradient in pore water. Because the former concentration gradient in the mixtures was nearly equal to that of adsorbed Cs, the diffusion of Cs in the mixtures was probably dominated by the concentration gradient of the Cs adsorbed on the mixtures. In addition, the effective/apparent diffusivity of ²³⁷Np(IV) and apparent diffusivity of ²⁴¹Am(III) and ⁶⁰Co(II) in the mixtures were determined in 0.3/0.03 mol l⁻¹ (NH₄)₂CO₃/Na₂S₂O₄ solution.

KEYWORDS: diffusion, caesium, bentonite, effective diffusivity, apparent diffusivity, surface diffusion, sand-bentonite barrier, radioactive waste storage.

During the storage of high-level radioactive waste in a deep geological isolation systems, long-lived ¹³⁵Cs (half life: 2.3×10^6 years) may leach from the waste packages and subsequently move through the surrounding buffer materials to the geosphere. Thus, the buffer materials are expected to form a low-

permeability barrier against groundwater flow and to retard the migration of ¹³⁵Cs by sorption. For this purpose, compacted sand-bentonite mixtures are considered as candidate buffer materials. Water permeability in sand-bentonite mixtures is so low that diffusion is the only possible mechanism for ¹³⁵Cs transport.

Fick's 1st law of diffusion was applied to the diffusion of ions in sand-bentonite mixtures. Two diffusivities, apparent diffusivity (D_a) and effective diffusivity (D_e), are used to describe the diffusive transport of radionuclides through engineered and natural barriers in radioactive waste management.

* E-mail: sawaguchi.takuma@jaea.go.jp

[†] Part of this study was funded by the Secretariat of Nuclear Regulation Authority, Nuclear Regulation Authority, Japan.

DOI: 10.1180/claymin.2013.048.2.19

When the concentration gradient is defined on the basis of the amount of diffusing species per unit volume of porous material, the proportional constant between the flux and the concentration gradient is called D_a . On the other hand, when the definition is based on the concentration of diffusing species in pore water, the proportional constant is D_e .

The driving force behind cation diffusion in bentonite mixtures is well known for Sr^{2+} . Eriksen & Jansson (1996) showed positive correlation between D_e and distribution coefficient (K_d), which is evidence for the contribution of surface diffusion or diffusion in the sorbed state. For Cs, on the other hand, plausible data on the driving force for diffusion in bentonite mixtures are not available. On the basis of the results of a through-diffusion experiment, Muurinen *et al.* (1987) reported that surface diffusion is the predominant Cs diffusion mechanism in compacted bentonite. In their experiment, however, steady state was not reached, and the results and conclusion are questionable. Yu & Neretnieks (1997) conducted a literature review, proposed diffusion coefficients of elements in compacted bentonite, and concluded that surface diffusion effects are found for Cs, Pa and Sr in low-ionic-strength waters. Their discussion was, however, based on the effective diffusivity that was indirectly estimated from D_a and K_d data. Okamoto *et al.* (1999) hinted at the contribution of surface diffusion by showing that

the D_a of Cs is independent of K_d . The scarce information on Cs is mainly because of the difficulties encountered in through-diffusion experiments or the extremely long times required for reaching steady-state diffusion.

In this study, through-diffusion experiments for Cs in compacted sand-bentonite mixtures were performed under several water compositions, expecting that the variation in the water composition can lead to variations in Cs sorptivity and in the driving force of diffusion. We examined whether the apparent diffusivity or the effective diffusivity was the fixed constant, namely the proportional constant between the diffusive flux and the concentration gradient driving diffusion. For comparison, the diffusivities of $^{237}\text{Np(IV)}$, $^{241}\text{Am(III)}$, and $^{60}\text{Co(II)}$ in the mixtures were also determined under $0.3/0.03 \text{ mol l}^{-1} (\text{NH}_4)_2\text{CO}_3/\text{Na}_2\text{S}_2\text{O}_4$ conditions through multitracer diffusion experiments.

EXPERIMENTAL

Through-diffusion experiments were carried out at various solution compositions. The acrylic diffusion cell used in this study is shown in Fig. 1. The experimental conditions are summarized in Table 1. The employed bentonite material was Kunigel VI (Kunimine Industries Co. Ltd.), with 46–49 wt.% Na-montmorillonite (Ito *et al.*, 1993). In the

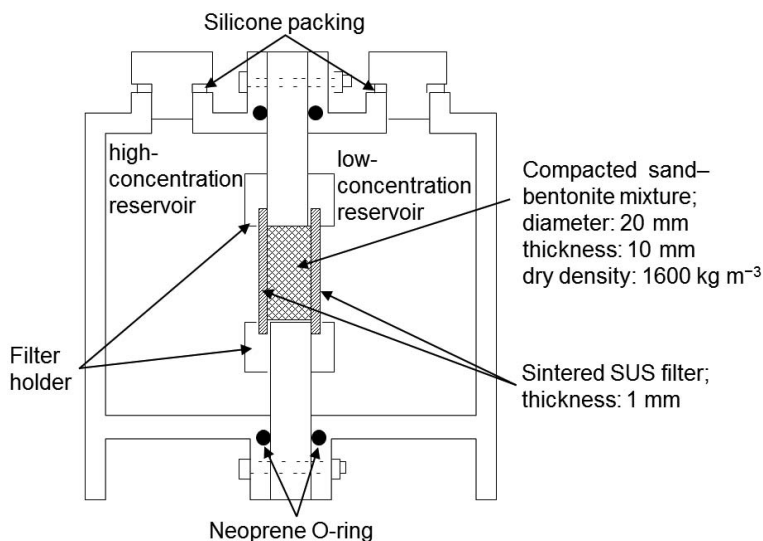


FIG. 1. Diffusion cell used in the through-diffusion experiments.

TABLE 1. Diffusion experimental results through compacted sand-bentonite mixtures.

Conditions	Species	K_d ($\text{m}^3 \text{kg}^{-1}$)	D_e ($\text{m}^2 \text{s}^{-1}$)	D_a ($\text{m}^2 \text{s}^{-1}$)	D_{eb} ($\text{m}^2 \text{s}^{-1}$)	Note
0.01 mol l ⁻¹ NaCl Ar atmosphere RT (25±3)°C	Cs ⁺	(1.0±0.2) × 10 ⁰	(5.9±1.7) × 10 ⁻⁹	(3.7±1.1) × 10 ⁻¹²	>5.9 × 10 ⁻⁹	Series-1–1, this study
0.5 mol l ⁻¹ NaCl Ar atmosphere RT (25±3)°C	Cs ⁺	(8.0±1.3) × 10 ⁻²	(6.7±1.6) × 10 ⁻¹⁰	(5.3±1.3) × 10 ⁻¹²	(7.8±2.8) × 10 ⁻¹⁰	Series-1–2, this study
0.5 mol l ⁻¹ NaOH Ar atmosphere RT (25±3)°C	Cs ⁺	(6.7±1.4) × 10 ⁻²	(6.7±2.2) × 10 ⁻¹⁰	(6.2±2.0) × 10 ⁻¹²	(7.8±4.0) × 10 ⁻¹⁰	Series-1–3, this study
(NH ₄) ₂ CO ₃ /Na ₂ S ₂ O ₄ , pH = 8.8 Total carbonate = 0.3 mol l ⁻¹ [S ₂ O ₄ ²⁻] = 0.03 mol l ⁻¹ <i>E</i> _H = -312 mV vs. NHE Ar atmosphere RT (26.4±2.7)°C	¹³⁷ Cs ⁺	(6.4±0.6) × 10 ⁻²	(5.2±0.5) × 10 ⁻¹⁰	(5.1±0.5) × 10 ⁻¹²	(5.6±0.7) × 10 ⁻¹⁰	Series-2, this study
		(6.0±0.3) × 10 ⁻²	(4.7±0.6) × 10 ⁻¹⁰	(4.9±0.6) × 10 ⁻¹²	(4.9±0.8) × 10 ⁻¹⁰	
		(6.8±0.2) × 10 ⁻²	(5.7±0.6) × 10 ⁻¹⁰	(5.2±0.6) × 10 ⁻¹²	(6.2±0.9) × 10 ⁻¹⁰	
		av. (6.4±0.7) × 10 ⁻²	av. (5.2±1.1) × 10 ⁻¹⁰	av. (5.1±0.8) × 10 ⁻¹²	av. (5.6±1.6) × 10 ⁻¹⁰	
	²³⁷ Np ^{IV} (CO ₃) ₂ (OH) ₂ ²⁻	(1.5±0.1) × 10 ⁻²	(4.3±0.4) × 10 ⁻¹¹	(1.8±0.2) × 10 ⁻¹²	(3.6±0.3) × 10 ⁻¹¹	
		(1.5±0.1) × 10 ⁻²	(4.1±0.4) × 10 ⁻¹¹	(1.7±0.2) × 10 ⁻¹²	(3.5±0.3) × 10 ⁻¹¹	
	(1.5±0.1) × 10 ⁻²	(4.5±0.5) × 10 ⁻¹¹	(1.8±0.2) × 10 ⁻¹²	(3.8±0.4) × 10 ⁻¹¹		
	²⁴¹ Am(CO ₃) ₃ ³⁻	–	–	1.7 × 10 ^{-14*}	–	
	⁶⁰ Co(NH ₃) ₆ ²⁺	–	–	7.6 × 10 ^{-15*}	–	
NaHCO ₃ /Na ₂ S ₂ O ₄ , pH = 9.0 Total carbonate = 0.3 mol l ⁻¹ [S ₂ O ₄ ²⁻] = 0.03 mol l ⁻¹ <i>E</i> _H = -430 to -250 mV vs. NHE Ar atmosphere RT (30°C)	¹³⁴ Cs ⁺	(2.6±0.3) × 10 ⁻¹	(9.3±1.1) × 10 ⁻¹⁰	(2.2±0.3) × 10 ⁻¹²	(1.2±0.2) × 10 ⁻⁹	Yamaguchi <i>et al.</i> (2007)
		(2.7±0.3) × 10 ⁻¹	(8.8±0.9) × 10 ⁻¹⁰	(2.1±0.2) × 10 ⁻¹²	(1.1±0.2) × 10 ⁻⁹	Re-estimated, this study
		(2.1±0.3) × 10 ⁻¹	(7.0±0.8) × 10 ⁻¹⁰	(2.0±0.2) × 10 ⁻¹²	(7.9±1.3) × 10 ⁻¹⁰	
		av. (2.5±0.7) × 10 ⁻¹	av. (8.4±2.2) × 10 ⁻¹⁰	av. (2.1±0.4) × 10 ⁻¹²	av. (1.0±0.4) × 10 ⁻⁹	

The errors were evaluated at a confidence limit of 68% (1σ).

* Apparent diffusivity estimated by the distribution of species in the bentonite mixture at the end of the experiments.

experiments, mixtures of Kunigel V1 and silica sand were compacted to an acrylic diffusion column of 20 mm in diameter and 10 mm in thickness. The mixture ratio of Kunigel V1 and silica sand was 7:3 by dry weight and the density of the mixed specimens was 1600 kg m^{-3} ; these are specified as the reference buffer material in Japan (JNC, 2000). Each side of the sand-bentonite mixture was covered with sintered stainless steel, 1-mm-thick filters of 40% porosity in order to prevent the expansion of bentonite in the reservoirs.

Series-1-1: 0.01 mol l⁻¹ NaCl solution

A multitracer through-diffusion experiment was performed by using the diffusion cell following a diffusion experiment for HTO. A 0.01 mol l⁻¹ NaCl solution was employed to simulate fresh groundwater. The diffusion cell was soaked in the solution under vacuum to remove all air from the pores in the specimen. The two reservoirs of the diffusion cell were then filled with 1.1×10^{-1} l of the solution. The diffusion experiment was started by adding HTO to the solution in one of the reservoirs (high-concentration reservoir). At intervals of seven days, 1.0×10^{-3} l aliquot was taken from the low-concentration reservoir, and 1.0×10^{-4} l aliquot from the high-concentration reservoir for radiometric analysis. The 1.0×10^{-3} l aliquot removed from the low-concentration reservoir was replaced by an equal volume of 0.01 mol l⁻¹ NaCl solution to maintain the water levels in the two reservoirs. This balancing act prevents the development of a pressure difference that can lead to advective transport from the high-concentration to low-concentration reservoir. The concentrations of HTO in both reservoirs were determined by liquid scintillation counting (LS-6500, Beckman Coulter, Inc.). After the diffusion of HTO reached a steady state, the solution was replaced by one containing Cs, I, Ni, Sr, Nb, Sn and Pb in order to allow the elements to diffuse. The solutions were sampled, using a similar procedure to that in the HTO experiment, for 363 days. The concentrations of the elements were determined by using inductively coupled plasma-mass spectrometry (ICP-MS, JMS-PLASMAX2, JEOL Ltd.). The initial concentrations of HTO, Cs, I, Sr, and Sn were 100 kBq l⁻¹, 1×10^{-4} mol l⁻¹, 1×10^{-4} mol l⁻¹, 3×10^{-3} mol l⁻¹, and 6×10^{-5} mol l⁻¹, respectively. Because the concentrations of Ni, Nb and Pb were lower than the

detection limit, diffusivities were not obtained for these elements. The diffusion experiments were performed at room temperature under Ar ($\text{O}_2 < 1 \text{ ppm}$) to avoid oxidation of I⁻.

Series-1-2: 0.5 mol l⁻¹ NaCl solution

A 0.5 mol l⁻¹ NaCl solution was employed to simulate saline groundwater. The procedure of the diffusion experiments was similar to that of the series-1-1 experiments.

Series-1-3: 0.5 mol l⁻¹ NaOH solution

A 0.5 mol l⁻¹ NaOH solution was employed to simulate the highly alkaline groundwater conditions induced by cementitious materials in the radioactive waste repositories. The procedure of the diffusion experiments was similar to that of the series-1-1 experiments. In this series, the initial concentrations of HTO, Cs, I, Sr, Sn and Pb were 100 kBq l⁻¹, 1×10^{-4} mol l⁻¹, 2×10^{-4} mol l⁻¹, 1×10^{-3} mol l⁻¹, 1×10^{-4} mol l⁻¹ and 9×10^{-4} mol l⁻¹, respectively. The concentrations of Ni and Nb were lower than the detection limit, so the diffusivities were not determined.

Series-2: 0.3 mol l⁻¹ (NH₄)₂CO₃ solution

A 0.3 mol l⁻¹ (NH₄)₂CO₃ solution was used to simulate groundwater rich in ammonium, a reduction product of NO₃⁻ released from transuranic (TRU) waste. The diffusion cells were soaked in distilled-deionized water under vacuum to remove air from the pores of the specimens. Three diffusion cells (runs 1, 2 and 3) were filled with a 1.1×10^{-1} l (NH₄)₂CO₃/Na₂S₂O₄ mixed solution, whose total ammonia concentration, total carbonate concentration and dithionite concentration were 6.0×10^{-1} mol l⁻¹, 3.0×10^{-1} mol l⁻¹ and 3.0×10^{-2} mol l⁻¹, respectively. A diffusion cell without bentonite was used in a blank test to check the adsorption of radionuclides on the cell walls. The diffusion cells were transferred into an atmosphere-controlled glove box and left for 30 days to condition the specimens in the solution. The starting solution was prepared by combining a 5.5×10^{-1} l of (NH₄)₂CO₃/Na₂S₂O₄ solution, a 1.0×10^{-5} l ¹³⁷Cs stock solution, a 9.0×10^{-4} l ⁶⁰Co stock solution, a 1.0×10^{-4} l ²⁴¹Am stock solution and a 1.5×10^{-3} l Np(IV) stock solution in a polypropylene bottle. The concentrations of NH₄⁺, HCO₃⁻, S₂O₄²⁻, ¹³⁷Cs, ⁶⁰Co, ²⁴¹Am,

and ^{237}Np in the starting solution were 0.6 mol l^{-1} , 0.3 mol l^{-1} , 0.03 mol l^{-1} , $5.5 \times 10^1 \text{ kBq l}^{-1}$, $5.5 \times 10^1 \text{ kBq l}^{-1}$, $1.35 \times 10^2 \text{ kBq l}^{-1}$ and $1.36 \times 10^2 \text{ kBq l}^{-1}$, respectively. The pH and E_{H} (redox potential against normal hydrogen electrode) of the solutions were measured with electrodes. Aliquots of the solutions were withdrawn to determine the concentrations of radionuclides by γ -spectrometry. The diffusion runs started by replacing the solution in one of the reservoirs with a $1.1 \times 10^{-1} \text{ l}$ starting solution and a blank test with a $2.2 \times 10^{-1} \text{ l}$ starting solution. At intervals of three weeks, the solutions in the high- and low-concentration reservoirs were sampled. The sampling procedure was similar to the series-1 experiments.

After performing series-2 diffusion runs for 363 days, a series of post-experimental analyses were performed for the diffusion tests and the blank test. The pH and E_{H} were measured with electrodes, and the ratio of Np(IV) to the total dissolved Np was determined using the thenoyltrifluoroacetone (TTA) extraction technique (Yamaguchi *et al.*, 2007). Np(IV) is extracted by TTA, while the other oxidation states of Np remain in the aqueous phase (Foti & Freiling, 1964) in $1 \text{ mol l}^{-1} \text{ HCl}$. We filtered $4.0 \times 10^{-4} \text{ l}$ aliquots of the solution through four types of filters, a $0.45 \mu\text{m}$ durapore (PVDF, polyvinylidene fluoride) filter, a regenerated cellulose filter with 100 k and 30 k nominal molecular weight limit (NMWL), and polyether sulphon filters with 10 k and 5 k NMWL in series to analyse the colloidal Np in the solution. The filters were preconditioned by filtering a $4.0 \times 10^{-4} \text{ l}$ aliquot of the solution before use to avoid any change in the Np concentration during filtration. The remainder of the solution was removed from the reservoir and the diffusion cell was disassembled. Each reservoir was rinsed with $1.0 \times 10^{-2} \text{ l}$ deionized water three times, and then rinsed with $1.0 \times 10^{-2} \text{ l}$ of $1.0 \times 10^1 \text{ mol l}^{-1} \text{ HNO}_3$ to analyse the amount of Np adsorbed on the acrylic walls. The sand-bentonite mixture was pushed out from the acrylic frame one millimeter at a time by using a screw presser and sliced with a steel blade to reveal the distribution of radionuclides in the sand-bentonite mixture specimens. Because the periphery of the slice seemed to be disturbed from pushing the sample out of the acrylic frame, the centre of the slice with a 14 mm in diameter was cut using a polypropylene tube. The specimen was dried, weighed, and analysed for radionuclides by γ -spectrometry.

DATA ANALYSIS

Neretnieks (1980) applied the pore diffusion equation proposed for diffusion in macroporous media by Brakel & Heertjes (1974) for modelling D_a and D_e in rock matrix

$$D_a = D_v \delta \tau^{-2} / (1 + \rho K_d / \phi) = D_p / (1 + \rho K_d / \phi) = D_e / (\phi + \rho K_d) \quad (1)$$

where D_v is the diffusivity in the bulk solution ($\text{m}^2 \text{ s}^{-1}$), δ is the constrictivity of the pores (dimensionless), τ is the tortuosity of the pores (dimensionless), ϕ is the porosity of the diffusion medium (dimensionless), ρ is the bulk density of the diffusion medium (kg m^{-3}), K_d is the distribution coefficient ($\text{m}^3 \text{ kg}^{-1}$) and D_p is the pore diffusivity ($\text{m}^2 \text{ s}^{-1}$).

Fick's 1st law of diffusion is applied to model one-dimensional diffusion in the diffusion medium. If the linear sorption isotherm is assumed, D_a and D_e are defined as

$$J = -D_a \frac{dC}{dx} = -D_a (\phi + \rho K_d) \frac{dc}{dx} = -D_e \frac{dc}{dx} \quad (2)$$

where J is the diffusive flux ($\text{mol m}^{-2} \text{ s}^{-1}$ or $\text{Bq m}^{-2} \text{ s}^{-1}$), C is the amount of diffusing species per unit volume of the diffusion medium (mol m^{-3} or Bq m^{-3}), x is the length coordinate in the diffusion direction (m), and c is the concentration of the diffusing species in pore water (mol m^{-3} or Bq m^{-3}). In this paper, the gradient of C , dC/dx , is called the "apparent concentration gradient."

Because of equation 1, the two diffusivities D_a and D_e coexist in the field of radioactive waste management. However, we need to identify whether dC/dx or dc/dx drives diffusion and to use the corresponding diffusivity to model the diffusive mass transfer. For $\phi \ll \rho K_d$, equation 2 can be rewritten as

$$J = -D_a \rho K_d \frac{dc}{dx} \quad (3)$$

Then, D_a becomes the ratio of the diffusive flux to the concentration gradient of the species adsorbed on the diffusion medium ($\rho K_d dc/dx$). Yu & Neretnieks (1997) defined this ratio as surface diffusivity.

The rate of change of concentration at a point in one-dimensional systems assuming linear sorption is given by Fick's 2nd law of diffusion:

$$\frac{\partial c}{\partial t} = \frac{D_e}{\phi + \rho K_d} \frac{\partial^2 c}{\partial x^2} \quad (4)$$

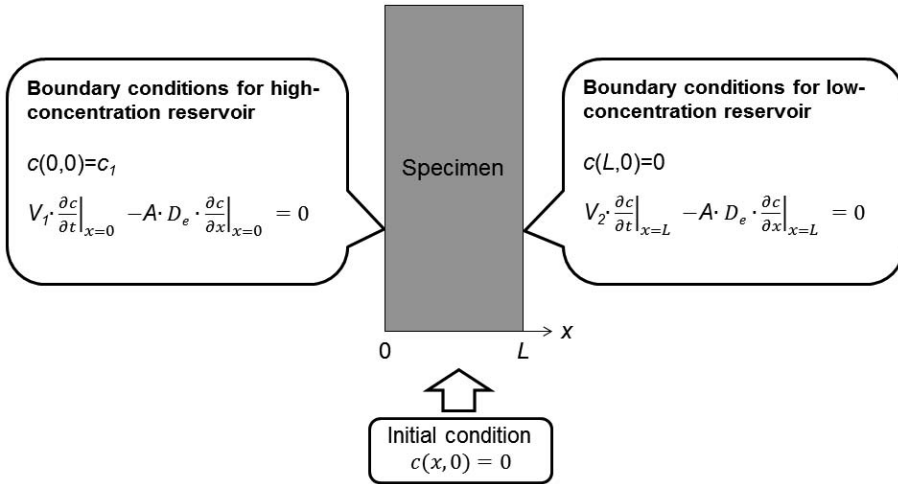


FIG. 2. Initial and boundary conditions for the through-diffusion experiments.

The exact solution of equation 4 for decreasing inlet concentration–increasing outlet concentration under the initial and boundary conditions shown in Fig. 2 was proposed by Zhang & Takeda (2005). The concentration of species at position x and time t is described using equation 5 (below). Where $\alpha = \phi + \rho K_d$, $\gamma = V_2 / V_1$, and $\beta = (\alpha AL) / V_1$. ϕ_m is calculated using equation 6:

$$\tan(\phi_m) = \frac{\beta \cdot (\gamma + 1) \cdot \phi_m}{\gamma \cdot \phi_m^2 - \beta^2} \quad (6)$$

where $c_1(0)$ is the concentration of species in the starting solution in the high-concentration reservoir (mol m⁻³ or Bq m⁻³), V_1 is the volume of the high-concentration reservoir (1.1 × 10⁻⁴ m³) and V_2 is the volume of the low-concentration reservoir (1.1 × 10⁻⁴ m³). The distribution coefficient was calculated using equation 7:

$$K_d = \frac{c_1(0) \cdot V_1 - c_{eq} \cdot (V_1 + V_2)}{c_{eq} \cdot M} \quad (7)$$

where c_{eq} is the concentration of species when the concentration gradient disappears (mol m⁻³ or

Bq m⁻³), and M is the dry weight of the diffusion medium (kg). The total column length including the filter was used in the analysis because the exact solution of the diffusion equation is available only for diffusion through a single domain. The effective diffusivity of the species was determined by fitting equation 5 to the concentrations of the species in the low-concentration reservoir. The apparent diffusivity was, on the other hand, estimated from D_e and K_d by using equation 1. Effective diffusivities in the sand-bentonite mixtures (D_{eb}) were determined by correcting for the loss of the concentration gradient in the filter by using equation 8: (Kato et al., 1999)

$$D_{eb} = \frac{L_b}{\frac{L}{D_e} - 2 \frac{L_f}{D_{ef}}} \quad (8)$$

where L_b is the column length of the sand–bentonite mixture (1.0 × 10⁻² m), L is the total column length including the filter thickness (1.2 × 10⁻² m), L_f is the filter thickness (1.0 × 10⁻³ m) and D_{ef} is the effective diffusivity of the species in the filter calculated by the pore diffusion model (4 × 10⁻¹⁰ m² s⁻¹).

$$c(x, t) = \frac{c_1(0)}{\beta + \gamma + 1} - 2c_1(0) \cdot \sum_{m=0}^{\infty} \frac{\exp\left(-\frac{D_e \cdot \phi_m^2}{\alpha \cdot L^2} \cdot t\right) \cdot \left[\beta \cdot \cos\left(\phi_m^2 \cdot \frac{L-x}{L}\right) - \gamma \cdot \phi_m \cdot \sin\left(\phi_m \cdot \frac{L-x}{L}\right)\right]}{\left[\gamma \cdot \phi_m^2 - \beta \cdot (\beta + \gamma + 1)\right] \cdot \cos(\phi_m) + \left[\beta \cdot \gamma + \beta + 2\gamma\right] \cdot \sin(\phi_m)} \quad (5)$$

We also applied the above-mentioned method to analyse the Cs diffusion data in a similar diffusion experiment using a 0.3/0.03 mol l⁻¹ NaHCO₃/Na₂S₂O₄ solution by Yamaguchi *et al.* (2007), and re-estimated D_e and D_a .

RESULTS AND DISCUSSION

Diffusivities of Cs

The changes in the concentrations of Cs in the high- and low-concentration reservoirs are shown in Fig. 3. The concentration of Cs in the low-concentration reservoir was first detected after 20–40 days, then gradually increased, and finally reached equilibrium about 150 days later. The concentrations of radioactive Cs have been compensated for radioactive decay in series-2. The distribution coefficients and diffusivities of Cs estimated using the exact solution are summarized in Table 1. The distribution coefficients of Cs⁺ in 0.01 mol l⁻¹ NaCl solution, 0.5 mol l⁻¹ NaCl solution, 0.5 mol l⁻¹ NaOH solution, 0.3/0.03 mol l⁻¹ (NH₄)₂CO₃/Na₂S₂O₄ solution and 0.3/0.03 mol l⁻¹ NaHCO₃/Na₂S₂O₄ solution were obtained as 1.0 m³ kg⁻¹, 0.080 m³ kg⁻¹, 0.067 m³ kg⁻¹, 0.064 m³ kg⁻¹ and 0.25 m³ kg⁻¹, respectively. The distribution coefficients of Cs⁺ decreased with increasing ionic strength.

At high ionic strength (series-1–2, series-1–3, series-2, and Yamaguchi *et al.*, 2007), the effective diffusivities through the column, including the filters, were corrected for the filter effect to obtain effective diffusivity through the specimens using equation 8. On the other hand, the effective diffusivity through the column for low ionic strength (series-1–1) was higher than the value expected when only the filter was placed in the column (2.4×10^{-9} m² s⁻¹), and could not be corrected using equation 8. The D_{eb} of Cs in series-1–1 shown in Table 1 is a minimum value.

Effective diffusivities of Cs⁺ in 0.01 mol l⁻¹ NaCl, 0.5 mol l⁻¹ NaCl, 0.5 mol l⁻¹ NaOH, 0.3/0.03 mol l⁻¹ (NH₄)₂CO₃/Na₂S₂O₄ and 0.3/0.03 mol l⁻¹ NaHCO₃/Na₂S₂O₄ solutions were obtained as $> 5.9 \times 10^{-9}$ m² s⁻¹, $(7.8 \pm 2.8) \times 10^{-10}$ m² s⁻¹, $(7.8 \pm 4.0) \times 10^{-10}$ m² s⁻¹, $(5.6 \pm 1.6) \times 10^{-10}$ m² s⁻¹ and $(1.0 \pm 0.4) \times 10^{-9}$ m² s⁻¹, respectively. The effective diffusivities of Cs⁺ were higher than those of HTO, which ranged from 1.5 to 2.0×10^{-10} m² s⁻¹ (JAEA, 2006).

The apparent diffusivities of Cs⁺ in 0.01 mol l⁻¹ NaCl, 0.5 mol l⁻¹ NaCl, 0.5 mol l⁻¹ NaOH, 0.3/0.03 mol l⁻¹ (NH₄)₂CO₃/Na₂S₂O₄ and 0.3/0.03 mol l⁻¹ NaHCO₃/Na₂S₂O₄ solutions were obtained as $(3.7 \pm 1.1) \times 10^{-12}$ m² s⁻¹, $(5.3 \pm 1.3) \times 10^{-12}$ m² s⁻¹, $(6.2 \pm 2.0) \times 10^{-12}$ m² s⁻¹, $(5.1 \pm 0.8) \times 10^{-12}$ m² s⁻¹ and $(2.1 \pm 0.4) \times 10^{-12}$ m² s⁻¹, respectively. The apparent diffusivities obtained in this study were close to those reported by Sato *et al.* (1992) and by Kozaki *et al.* (1999) from in-diffusion experiments using compacted montmorillonite. At the same effective montmorillonite density (montmorillonite gel density; Sawaguchi *et al.*, 2006) and temperature as in this study, their values were 8.0×10^{-12} m² s⁻¹ and 4.8×10^{-12} m² s⁻¹, respectively.

The diffusivities, D_e and D_a , as a function of K_d are shown in Figs 4 and 5, respectively. D_e values of 4.7×10^{-10} to 5.9×10^{-9} m² s⁻¹ were obtained with somewhat large variation. The variation is not caused by the variation in the geometry of the diffusion pathways because the density and mixture ratio of the sand-bentonite mixture specimens were the same in all diffusion runs. D_a values, on the other hand, varied less from 2.0×10^{-12} to 6.2×10^{-12} m² s⁻¹. The results indicate that the diffusive flux is proportional to the apparent concentration gradient of Cs⁺ in the compacted sand-bentonite mixtures rather than the gradient of the Cs⁺ concentration in pore water. Because the apparent concentration gradient in the mixture is nearly equal to the gradient of adsorbed Cs⁺, the diffusion of Cs⁺ in the mixtures is probably dominated by the concentration gradient of the Cs⁺ adsorbed on the mixtures. As shown in Fig. 4, the D_e of Cs⁺ is not constant but positively correlated to K_d , which may be explained if surface diffusion is dominant at high K_d and its contribution decreases as K_d decreases at high ionic strength. Figure 4, however, shows that the contribution of surface diffusion is almost equal to that of pore diffusion in 0.5 mol l⁻¹ solutions (series-1–2 and series-1–3), which are equivalent to saline groundwater.

Diffusivities of other elements

In series-2, Np was prepared as Np (IV) at the start of the diffusion and TTA extraction was 99% at the termination of the diffusion runs. Np (IV) is extracted by TTA, while the other oxidation states of Np remain in the aqueous phase. The pH, E_H,

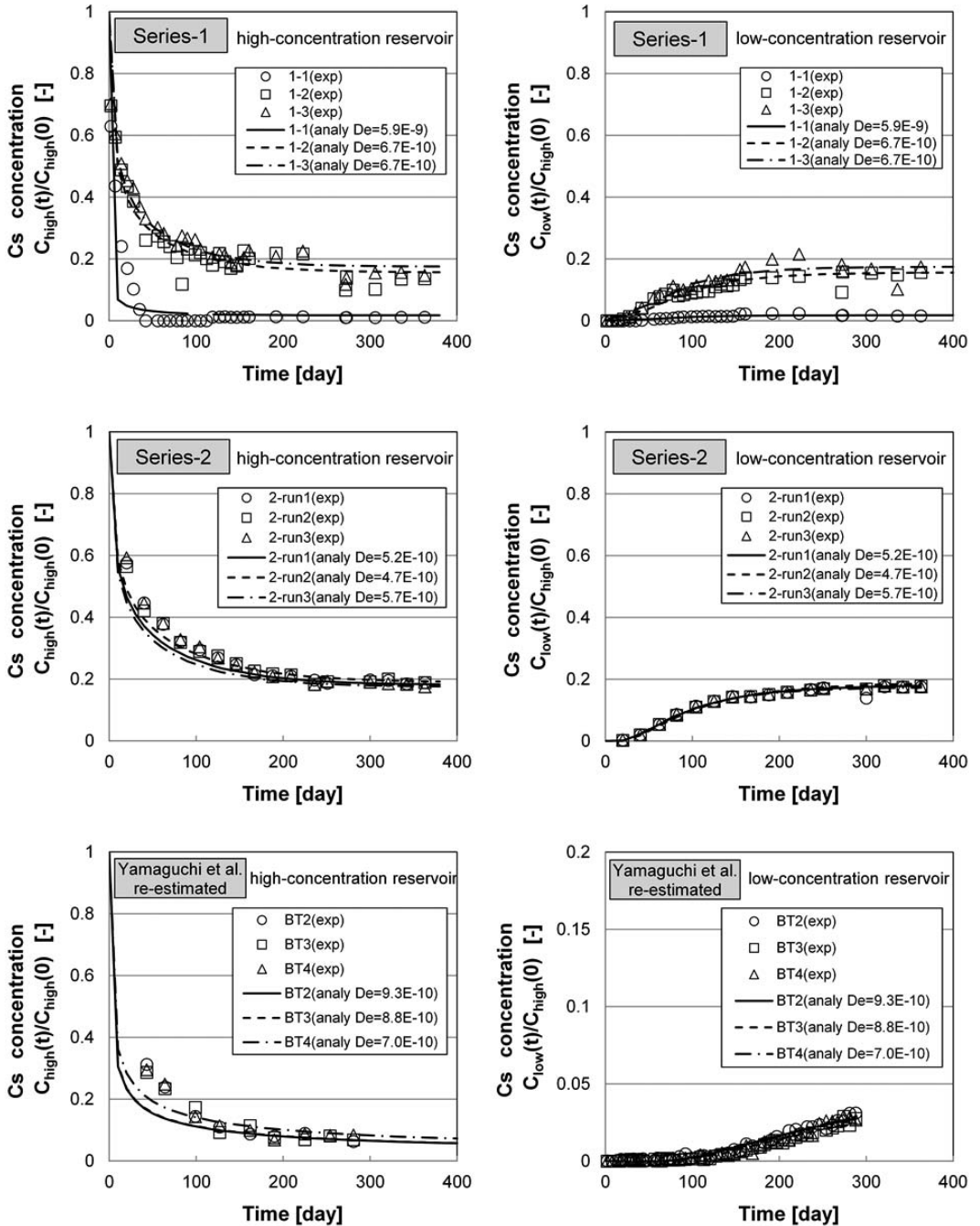


FIG. 3. Changes in the Cs concentrations of the high- and low-concentration reservoirs for series-1, series-2, and the diffusion data of Yamaguchi *et al.* (2007).

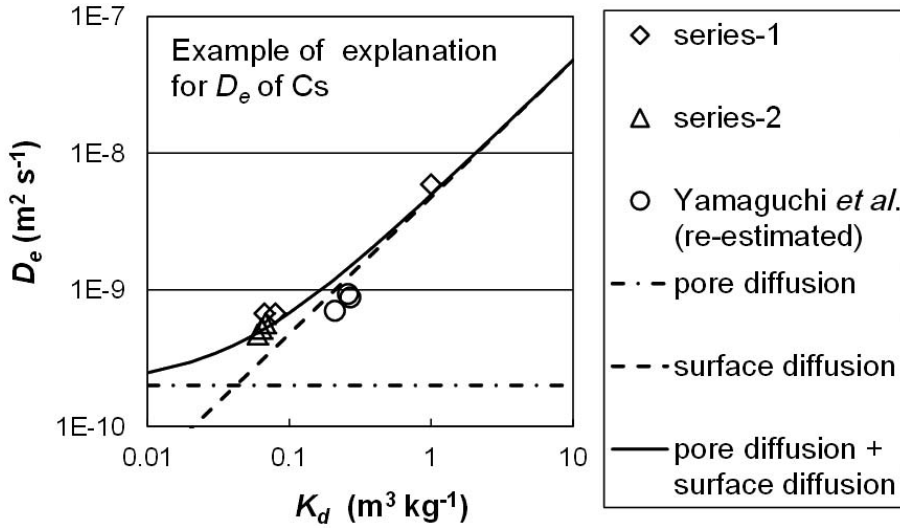


FIG. 4. Effective Cs diffusivities (D_e) in compacted sand-bentonite mixtures as a function of distribution coefficient (K_d). The lines show the least-squares fitting of the $D_e = \phi \cdot D_p + \rho \cdot K_d D_s$ equation (Yu & Neretnieks, 1997) to the data for a trial where $\phi \cdot D_p$ is $2.0 \times 10^{-10} \text{ m}^2 \text{ s}^{-1}$ (Yamaguchi *et al.*, 2007). D_s was $3.0 \times 10^{-12} \text{ m}^2 \text{ s}^{-1}$.

and total carbonate concentrations were 8.8, -312 mV vs. normal hydrogen electrode (NHE) and $3.0 \times 10^{-1} \text{ mol l}^{-1}$, respectively, at the termination of each diffusion run. These facts ensured that Np was mainly in the +IV state throughout the diffusion runs. The filtration analysis showed that (97%± 6%) of Np passed through the

5 k NMWL filter, which ensured that Np was not present in the solution as colloidal particles. Speciation calculations using a thermodynamic database (Yamaguchi, 2000) show that the carbonatohydroxo complex of $\text{Np}^{\text{IV}}(\text{CO}_3)_2(\text{OH})_2^{2-}$ accounts for most ratios of Np under the experimental conditions.

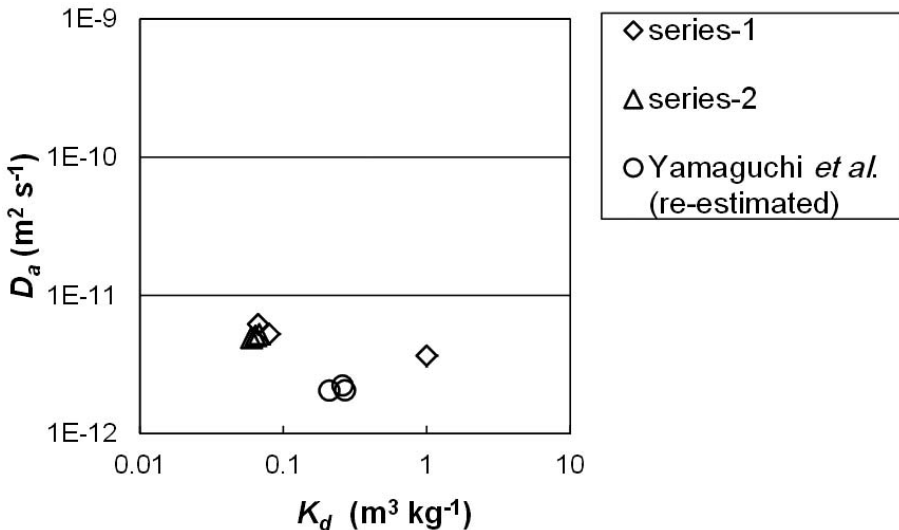


FIG. 5. Apparent Cs diffusivity (D_a) in compacted sand-bentonite mixtures as a function of the distribution coefficient (K_d).

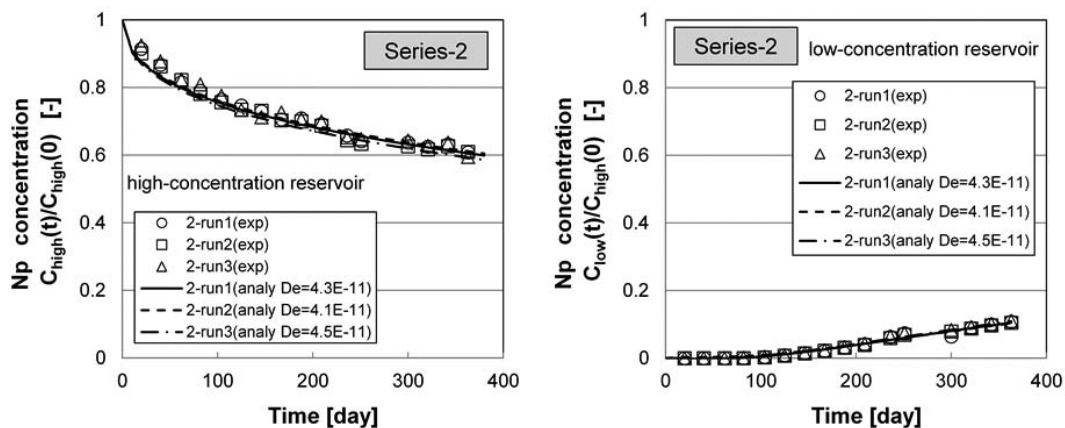


FIG. 6. Changes in Np concentrations in high- and low-concentration reservoirs for series-2.

The concentrations of ^{237}Np in the high-concentration reservoirs decreased throughout the experimental period of 363 days, as shown in Fig. 6. Np diffusion in the specimens reached a steady state after 300 days. The effective diffusivities of Np in series-2 were estimated using the exact solution (Table 1), and the analytical results reproduced well the experimental results in both reservoirs.

Under the above-mentioned solution conditions of series-2, it is assumed that ^{241}Am exists as $^{241}\text{Am}(\text{CO}_3)_3^{3-}$ and ^{60}Co as $^{60}\text{Co}(\text{NH}_3)_n^{2+}$. In this series, ^{241}Am and ^{60}Co were not detected in the low-concentration reservoirs during the whole experimental period. Mass balance calculations of ^{241}Am and ^{60}Co at the termination of the diffusion

runs (Table 2) show that they primarily existed in the filter and could precipitate in the high-concentration reservoirs because of the high loss. Therefore, their K_d and D_e could not be estimated with the exact solution. Hence, only D_a was calculated from the concentration distribution in the compacted mixtures by using the following equation: (Crank, 1975)

$$C(x, t) = \frac{A}{\sqrt{\pi D_a t}} \exp\left(-\frac{x^2}{4D_a t}\right) \quad (9)$$

where A is the amount of deposited species per unit area (mol m^{-2} or Bq m^{-2}). Figures 7 and 8 show the distributions of ^{241}Am and ^{60}Co in the bentonite mixture at the end of series-2 experiments and the

TABLE 2. Final distribution of Cs, Np, Am and Co in the series-2 experiments.

	– Cs –		– Np –		– Am –		– Co –	
	Bq	%	Bq	%	Bq	%	Bq	%
Total inventory	7813	100.0	27083	100.0	20303	100.0	6000	100.0
Solution in high-concentration reservoir	1529	19.6	17710	65.4	1474	7.3	46	0.8
Solution in low-concentration reservoir	1419	18.2	4554	16.8	0	0.0	0	0.0
Filter facing the high-concentration reservoir	3	0.0	63	0.2	2224	11.0	356	5.9
Filter facing the low-concentration reservoir	3	0.0	20	0.1	5	0.0	0	0.0
Wall of the high-concentration reservoir	2	0.0	6	0.0	36	0.2	151	2.5
Wall of the low-concentration reservoir	2	0.0	0	0.0	0	0.0	0	0.0
Sand-bentonite mixture	2944	37.7	6219	23.0	9689	47.7	306	5.1
Loss*	1911	24.5	–1490	–5.5	6875	33.9	5140	85.7

* Calculated by subtracting the analysed final inventory from the total amount used in the experiment.

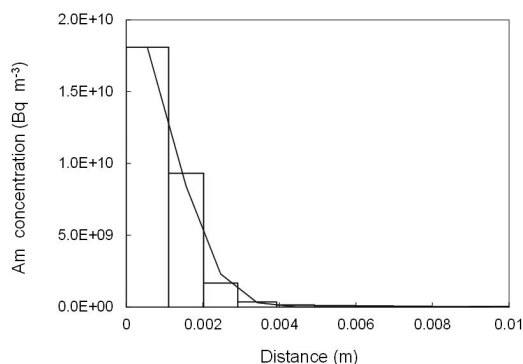


FIG. 7. Distribution of americium-241 in the bentonite mixture at the end of the series-2 experiments and the results of the least-squares fitting.

results of the least-squares fitting, respectively. The apparent diffusivity of $^{241}\text{Am}(\text{CO}_3)_3^{3-}$ in the 0.3/0.03 mol l^{-1} $(\text{NH}_4)_2\text{CO}_3/\text{Na}_2\text{S}_2\text{O}_4$ solution was $1.7 \times 10^{-14} \text{ m}^2 \text{ s}^{-1}$ and that of $^{60}\text{Co}(\text{NH}_3)_n^{2+}$ was $7.6 \times 10^{-15} \text{ m}^2 \text{ s}^{-1}$.

The effective diffusivities of HTO, I, Ni, Sr, Nb, Sn and Pb in the series-1 experiments are described elsewhere (JAEA, 2006). Further investigation is necessary to identify the driving force behind the diffusion of elements other than Cs and Sr.

CONCLUSION

The driving force for the diffusion of Cs^+ through compacted sand-bentonite mixtures was studied using the through-diffusion method under different aqueous compositions. The variation in effective diffusivity values was somewhat large, while that in

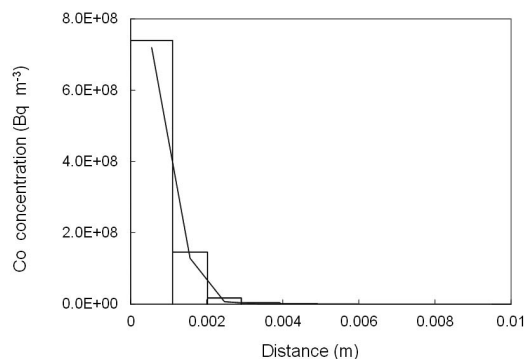


FIG. 8. Distribution of cobalt-60 in the bentonite mixture at the end of the series-2 experiments and the results of the least-squares fitting.

the apparent diffusivity values was small. The results indicated that the diffusion of Cs in the adsorbed state would be the main Cs diffusion mechanism in the mixtures.

ACKNOWLEDGMENTS

The authors acknowledge Messrs M. Kizaki, S. Miyata, Y. Kawasaki and F. Itonaga for performing the long-term experiments at the Waste Safety Testing Facility (WASTEF) of the Japan Atomic Energy Agency. Messrs N. Ito, S. Inagaki and T. Kawamura are acknowledged for the caesium concentration analyses by ICP-MS. Professor Ivars Neretnieks and an anonymous referee are acknowledged for reviewing the manuscript and making helpful comments.

REFERENCES

- Brakel J.V. & Heertjes P.M. (1974) Analysis of diffusion in macroporous media in terms of a porosity, a tortuosity and a constrictivity factor. *International Journal of Heat and Mass Transfer*, **17**, 1093–1103.
- Crank J. (1975) *The Mathematics of Diffusion*, 2nd edition, p. 13. Clarendon Press, Oxford.
- Eriksen T.E. & Jansson M. (1996) *Diffusion of Γ^- , Cs^+ and Sr^{2+} in compacted bentonite – Anion exclusion and surface diffusion*. SKB Technical Report 96-16, Swedish Nuclear Fuel and Waste Management Company.
- Foti S.C. & Freiling E.C. (1964) The determination of the oxidation states of tracer uranium, neptunium and plutonium in aqueous media. *Talanta*, **11**, 385–392.
- Ito M., Okamoto M., Shibata M., Sasaki Y., Danhara T., Suzuki K. & Watanabe T. (1993) *Mineral Composition Analysis of Bentonite*. PNC TN 8430 93-003, Power Reactor and Nuclear Fuel Development Corporation [in Japanese].
- JAEA (2006) H17 Research on long-term safety assessment methodology for radioactive waste disposal – Research on probabilistic approach to long-term safety assessment methodology. Japan Atomic Energy Agency [in Japanese].
- JNC (2000) H12 Project to Establish the Scientific and Technical Basis for HLW Disposal in Japan, Project Overview Report, 2nd Progress Report on Research and Development for the Geological Disposal of HLW in Japan. JNC Technical Report TN1410 2000-001, Japan Nuclear Cycle Development Institute.
- Kato H., Nakazawa T., Ueta S. & Yato T. (1999) Measurements of effective diffusivities of tritiated water in sand-mixed bentonite. *Proceedings of the 7th International Conference on Radioactive Waste*

- Management and Environmental Remediation-ASEM 1999*, Nagoya, Japan, September 26-30, 1999.
- Kozaki T., Sato H., Sato S. & Ohashi H. (1999) Diffusion mechanism of cesium ions in compacted montmorillonite. *Engineering Geology*, **54**, 223–230.
- Muurinen A., Penttilä-Hiltunen P. & Rantanen J. (1987) Diffusion mechanisms of strontium and cesium in compacted sodium bentonite. Pp. 803–812 in: *Scientific Basis for Nuclear Waste Management X, Materials Research Society Symposium Proceedings* (J.K. Bates & W.B. Seefeldt, editors), **84**.
- Neretnieks I. (1980) Diffusion in the rock matrix: an important factor in radionuclide retardation? *Journal of Geophysical Research*, **85**, 4379–4397.
- Okamoto A., Idemitsu K., Furuya H., Inagaki Y. & Arima T. (1999) Distribution coefficients and apparent diffusion coefficients of cesium in compacted bentonites. Pp. 1091–1098 in: *Materials Research Society Symposium*, **556**, *Scientific Basis for Nuclear Waste Management*, 22 (W. David & J.H. Lee, editors).
- Sato H., Ashida T., Kohara Y., Yui M. & Sasaki N. (1992) Effect of dry density on diffusion of some radionuclides in compacted sodium bentonite. *Journal of Nuclear Science and Technology*, **29**, 873–882.
- Sawaguchi T., Takeda S., Kozaki T., Sekioka Y., Kato H. & Kimura H. (2006) Assessment of data uncertainty on the diffusion coefficients for nuclides in engineered and natural barriers. Pp. 21–26 in: *JAEA-Conf 2008-001, Proceedings of the International Information Exchange Meeting on Diffusion Phenomena in Bentonite and Rock; Aiming at the Safety Assessment of the Geological Disposal* (H. Sato & K. Hatanaka, editors), July 18, 2006, Horonobe, Japan.
- Yamaguchi T. (2000) Consideration of thermodynamic data for predicting solubility and chemical species of elements in groundwater. Part 2: Np, Pu. JAERI-Data/Code 2000-031, Japan Atomic Energy Research Institute [in Japanese].
- Yamaguchi T., Nakayama S., Nagao S. & Kizaki M. (2007) Diffusive transport of neptunium and plutonium through compacted sand-bentonite mixtures under anaerobic conditions. *Radiochimica Acta*, **95**, 115–125.
- Yu J-W. & Neretnieks I. (1997) *Diffusion and sorption properties of radionuclides in compacted bentonite*. SKB Technical Report 97-12, Swedish Nuclear Fuel and Waste Management Company.
- Zhang M. & Takeda M. (2005) Theoretical evaluation of the through-diffusion test for determining the transport properties of geological materials. *Proceedings of Waste Management Symposium 2005*, February 27–March 3, 2005, Tucson, Arizona, USA.